

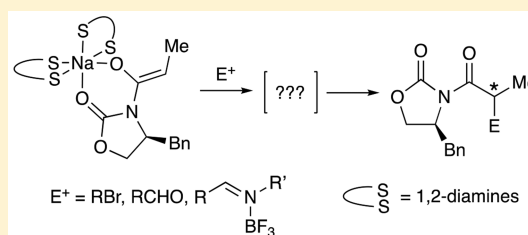
Structures and Reactivities of Sodiated Evans Enolates: Role of Solvation and Mixed Aggregation on the Stereochemistry and Mechanism of Alkylations

Zirong Zhang¹ and David B. Collum*¹

Department of Chemistry and Chemical Biology Baker Laboratory, Cornell University, Ithaca, New York 14853-1301, United States

Supporting Information

ABSTRACT: Oxazolidinone-based sodiated enolates (Evans enolates) were generated using sodium diisopropylamide (NaDA) or sodium hexamethyldisilazide (NaHMDS) in the presence of *N,N,N',N'*-tetramethylethylenediamine (TMEDA), (*R,R*)-*trans*-*N,N,N',N'*-tetramethylcyclohexanediamine [(*R,R*)-TMCDA], or (*S,S*)-TMCDA. ¹³C NMR spectroscopic analysis in conjunction with the method of continuous variations (MCV), x-ray crystallography, and density functional theory (DFT) computations revealed the enolates to be octahedral *bis*-diamine-chelated monomers. Rate and computational studies of an alkylation with allyl bromide implicate a *bis*-diamine-chelated-monomer-based transition structure. The sodiated Evans enolates form mixed dimers with NaHMDS, NaDA, or sodium 2,6-di-*tert*-butylphenolate, the reactivities of which are examined. Stereoselective quaternizations, aldol additions, and azaaldol additions are described.



INTRODUCTION

Oxazolidinone-derived enolates—so-called Evans enolates—have been used in both academic and industrial laboratories in the development of asymmetric syntheses since they were first reported by Evans and co-workers in 1981.¹ Highly stereoselective functionalizations stemming from a wide variety of auxiliaries and counterions are legion.² Aldol additions typically rely on boron- or transition-metal-based enolates,³ whereas alkylations require the more reactive sodium and lithium enolates.^{1,4}

We previously characterized the structures of lithiated Evans enolates as tetramer–dimer mixtures in tetrahydrofuran (THF) solution,⁵ underscored potential applications in simple aldol additions,^{6,7} and demonstrated doubly diastereoselective aldol additions using lithium enolate–lithium amino alkoxide mixed tetramers.⁸ We have also examined the structures and reactivities of key intermediates in di-*n*-butylboron triflate-based aldol additions.^{9,10}

This paper examines the corresponding sodium enolates. Sodium enolate **2** in neat THF shows broad ¹H and ¹³C resonances reminiscent of the poor structural control of simple sodium enolates in THF solution.¹¹ Although the use of THF is prevalent throughout organolithium chemistry,^{12,13} could it be that the almost irresistible urge to use THF as the default medium may be suboptimal for organosodium compounds?

Structural, mechanistic, and stereochemical studies of sodiated Evans enolates generically depicted as **2** (eq 1) in toluene solutions with *N,N,N',N'*-tetramethylethylenediamine (TMEDA) and related *N,N,N',N'*-tetramethylcyclohexanediamines [(*R,R*)- and (*S,S*)-*trans*-TMCDA] reveal octahedral monomers of general structure **4** (Chart 1). Moreover, vicinal diamines promote mixed dimers **5–7**. Studies of the structure

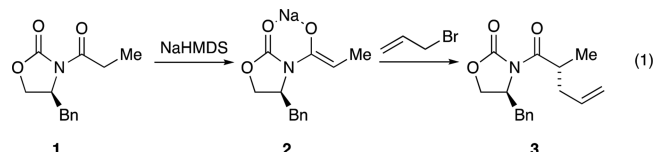
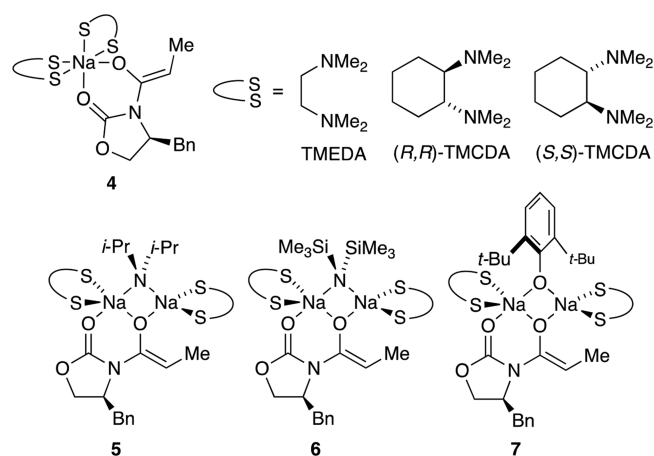


Chart 1. Structures of Sodiated Evans Enolates Solvated by Diamines



and mechanism of alkylation are shaping our thinking about the ligand-based control of structure and selectivity in

Received: September 25, 2018

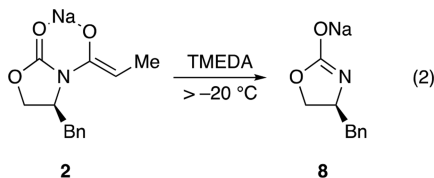
Published: November 21, 2018

organosodium chemistry, and the results underscore the potential merits of diamine/hydrocarbon mixtures.

RESULTS

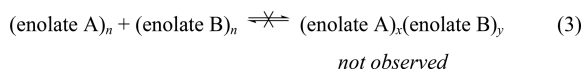
General Methods. Sodium enolates were generated using either NaDA^{14,15} or sodium hexamethyldisilazide (NaHMDS)^{16,17} (recrystallized) dissolved in diamine/toluene solutions. Although the two bases afford similar results, NaHMDS is superior in this case owing to its ease of handling, commercial availability, and in some cases, superior role in subsequent functionalizations stemming from reversible deprotonation. Structures and reaction coordinates were examined with density functional theory (DFT) computations at the B3LYP/6-31G(d) level of theory with single-point calculations at the MP2 level of theory.¹⁸ We refer to generic enolate **2** and the more specific monomer **4** interchangeably, depending on the context.

Enolization with either 0.10 M NaDA or 0.10 M NaHMDS in 1.0 M TMEDA/toluene is essentially instantaneous at -78 °C. The IR spectra show the loss of **1** at 1783 cm^{-1} and the appearance of an absorbance at 1743 cm^{-1} . During rate studies of alkylations, however, IR spectroscopy proved to have limited value owing to mediocre resolution and distortions caused by the deposition of NaBr. Also of note, sodium enolate **2** shows none of the aggregate-derived aging effects that can plague the highly aggregated lithium enolates.^{5,6} However, **2** decomposes above -20 °C, affording sodium salt **8** observed with in situ IR spectroscopy (eq 2; 1666 cm^{-1}).¹⁹ Deacylated oxazolidinone



along with debris that may derive from ketene were isolated on workup.^{2b} The decomposition is approximately 2-fold slower in TMEDA/toluene than in THF solutions, which may be more consequential than one might suspect (*vide infra*).

Structures of Enolate Monomers. ¹H and ¹³C NMR spectroscopic studies of enolate **2** in the absence of excess NaDA or NaHMDS showed resonances corresponding to a single magnetically distinct subunit, as observed by monitoring the ¹³C resonances of the oxazolidinone carbonyl carbon and the oxygen-bearing enolate carbon ($\delta 157.3$ and 152.7 ppm, respectively; Figure 1A). The diamine-solvated enolate was suggested to be monomeric when a synthetic racemate derived from (*S*)-**2** and (*R*)-**2** showed no resonances attributable to a heterochiral aggregate. Mixtures containing 1:1 pairs of enolate **2** with structurally analogous but spectroscopically distinct enolates **9a–d** as well as pairs containing **10** (six pairs in total) also showed no evidence of heteroaggregates (eq 3).²⁰ Emblematic ¹³C NMR spectra of a binary mixture are shown in Figure 1B,C. Heteroaggregates were also not formed from enolate pairs solvated by either (*S,S*)-TMEDA or (*R,R*)-TMEDA.



At the outset, we presumed that the monomers were four-coordinate chelates of general structure **11**. However, binary

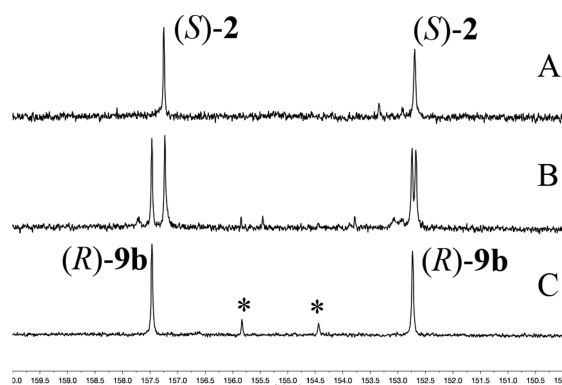
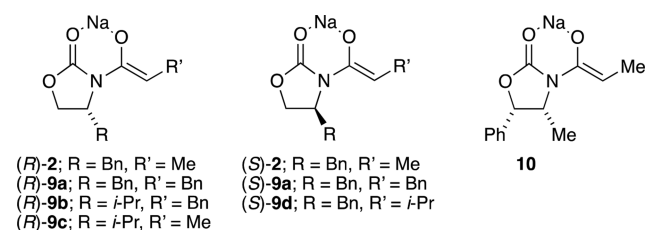


Figure 1. Partial ¹³C NMR spectra of a mixture (*S*)-**2** and (*R*)-**9b** (with 0.20 M total enolate titer) in 1.0 M TMEDA in toluene recorded at -80 °C: (A) pure (*S*)-**2**; (B) equimolar (*S*)-**2** and (*R*)-**9b**; (C) pure (*R*)-**9b**. *Denotes the enolate–NaHMDS mixed aggregate **6**.



mixtures of diamines afforded homo- and heterosolvates (eq 4) that could be resolved by ¹³C NMR spectroscopy, as shown in Figure 2. The peak broadening in the samples containing

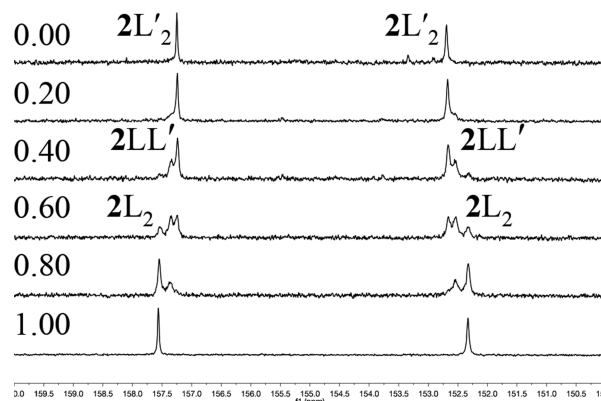


Figure 2. Partial ¹³C NMR spectra of a mixture with 0.20 M enolate **2** and 1.0 M total TMEDA (L) and (*S,S*)-TMEDA (L') concentration in toluene at -80 °C showing *bis*-TMEDA-solvated monomer ($2L_2$), *bis*-TMCDAsolvated monomer ($2LL'$; see eq 4). The *intended* mole fractions for TMEDA, X_{TMEDA} , are as labeled.

mixed solvates is consistent with stereoisomerism delineated in the Discussion. Despite the substandard spectral quality, we could use the method of continuous variations (MCV)²¹ to confirm the structure as a doubly TMEDA-chelated monomer. Varying the diamine proportions in TMEDA/(*S,S*)-TMEDA mixtures and monitoring the homo- and heterosolvates versus *measured* mole fraction of TMEDA (χ_{TMEDA}) afforded a Job plot²² with a unexpectedly good fit to the disolvate model (Figure 3).

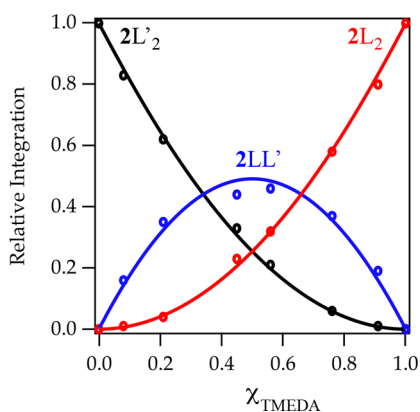
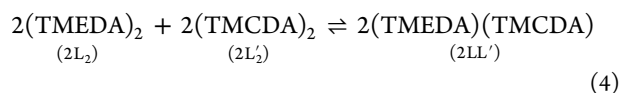
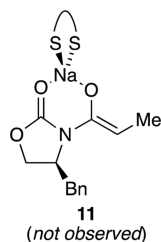


Figure 3. Job plot showing the relative integrations of *bis*-TMEDA-solvated monomer (2L₂), *bis*-TMEDA-solvated monomer (2L'₂), and mixed solvated monomer (2LL') versus the *measured* mole fraction of TMEDA for 0.20 M enolate (2) and TMEDA/(*S,S*)-TMEDA mixtures (1.0 M total diamine concentration) in toluene at $-80\text{ }^{\circ}\text{C}$.

MCV can present a dangerous trap, exemplified by the Job plot in Figure 3, that is worthy of elaboration. Using measured mole fraction—the mole fraction determined by monitoring only ligand within the ensemble of interest—eliminates distortions arising from measuring errors, impurities, and side equilibria. It also precludes the influence of binding constant on the position of maxima.²¹ By contrast, using the standard approach of plotting integration versus *intended* mole fraction—the mole fraction of the amines added within the total sample—provides the decidedly different result shown in Figure 4. It might be tempting to conclude from Figure 4 that TMEDA and (*S,S*)-TMEDA bind in a 2:1 stoichiometry. In this case, however, the skewing of the maximum to higher χ_{TMEDA} reflects the higher binding affinity of (*S,S*)-TMEDA relative to that of TMEDA.

One can (and we have²³) extract binding constants from such Job plots. (*S,S*)-TMEDA shows a -0.5 kcal/mol (exothermic) preference for substituting the first TMEDA and an attenuated -0.2 kcal/mol preference for substituting the second TMEDA. Computations predict -0.7 kcal/mol and -0.1 kcal/mol , respectively. Had the differential binding been more dramatic, the maximum would have been pushed even closer to the right-hand *y*-axis. An analogous Job plot shows that sequential substitutions of TMEDA by (*R,R*)-TMEDA are nearly thermoneutral ($+0.1$ and -0.1 kcal/mol , respectively).

Summarizing an important point, using a simple binary system in which two species, A and B, bind to each other poses no lurking risk because the relative binding constants are *by definition* identical: the maximum in the curve reflects the relative stoichiometries. If two species—ligands in this case—

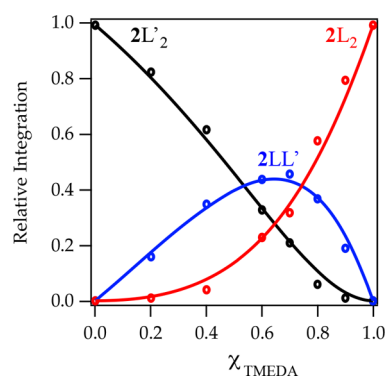


Figure 4. Job plot showing the relative integrations versus the *intended* mole fraction of TMEDA for a mixture of 0.20 M of enolate 2 and 1.0 M total diamine concentration in TMEDA/(*S,S*)-TMEDA mixtures in toluene at $-80\text{ }^{\circ}\text{C}$. The shift in the maximum to $\chi_{\text{TMEDA}} > 0.50$ reflects the stronger binding of (*S,S*)-TMEDA.

compete for binding to a third entity (sodium), however, differential binding eliminates the relationship of the maximum and the stoichiometry of binding. This risk has inspired one group to declare the “death of the Job plot.”²⁴ Although we think that declaration is a bit hyperbolic, such concerns should be heeded.

The veracity of the assignment of enolate 2 as the *bis*-chelated octahedral monomer 4 is supported by DFT computations showing the exothermic serial solvation of unsolvated enolate monomer 2 (eq 5). The octahedral geometry is illustrated in Figure 5 using the lowest energy

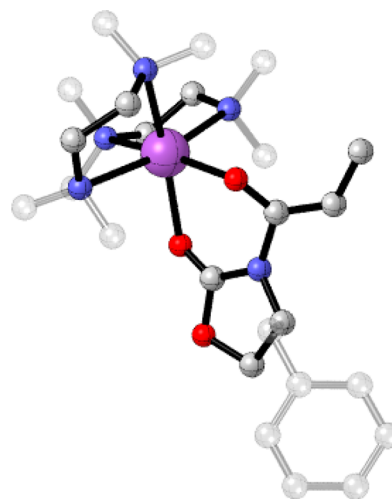
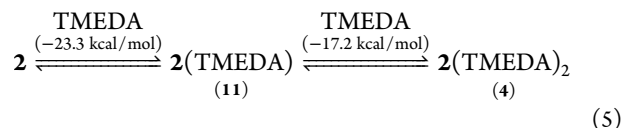


Figure 5. Computed structure of *bis*-chelated monomer 4 as its lowest energy δ stereoisomer.

stereoisomer of 4. A more elaborate description of the stereochemistry of chelation is deferred to the discussion.



Structures of Enolate–Amide Mixed Dimers. The enolization of 1 with excess NaDA or NaHMDS generates additional enolate ¹³C resonances manifesting amide-concentration-dependent intensities and amide-dependent chemical shifts (Figure 6). These new species are assigned as mixed

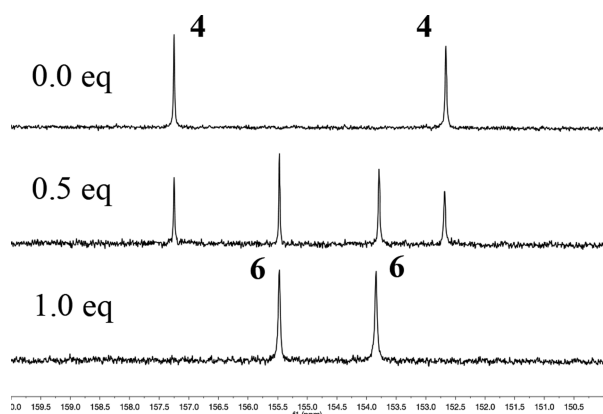


Figure 6. Partial ^{13}C NMR spectra of 0.20 M enolate **2** and 1.0 M TMEDA at various equivalents of excess NaHMDS (as indicated) in toluene at -80°C showing monomer **4** and mixed dimer **6**.

dimers **5** and **6**. The 1:1 stoichiometry in **6** is shown by the quantitative formation with 1.0 equiv of NaHMDS (Figure 6) as reflected in the Job plot in Figure 7. By contrast, NaDA

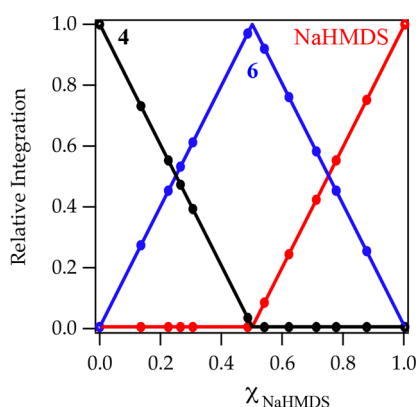


Figure 7. Job plot showing the relative integrations of NaHMDS (red), enolate monomer **4** (black), and mixed dimer **6** (blue) versus the measured mole fraction of NaHMDS with various proportions of NaHMDS and enolate (0.30 M total sodium titer) in 0.60 M TMEDA/toluene at -80°C . The ratios were ascertained by following the resonances of monomer **4** (carbonyl carbon at $\delta 157.3$), mixed dimer **6** (carbonyl carbon at $\delta 155.5$ and Me_3Si carbon at $\delta 7.52$), and NaHMDS (Me_3Si carbon $\delta 6.76$ ppm).

shows qualitatively similar behavior, albeit reflecting a soft equilibrium (Figures 8 and 9). Thus, NaHMDS shows a greater penchant than NaDA for mixed aggregation, which is the opposite of what is observed for LDA and LiHMDS.²⁵

We attempted to confirm the number of chelating ligands on mixed dimers **5** and **6** by integrating the ^{13}C resonances of free and bound TMEDA, but we were unable to obtain the necessary resolution. Nonetheless, decreasing the TMEDA concentration promotes NaDA mixed dimer **5**, consistent with a lower per-sodium solvation (eq 6).^{15,26} DFT computations using the NaHMDS-derived mixed dimer **6** emblematically showed serial chelation by TMEDA to be exothermic for both the first and the second ligations (Scheme 1). The computed structure of the bis-chelate is illustrated in Figure 10. The planes defined by Na_2O_2 and the oxazolidinone chelated enolate are twisted by $50\text{--}60^\circ$.

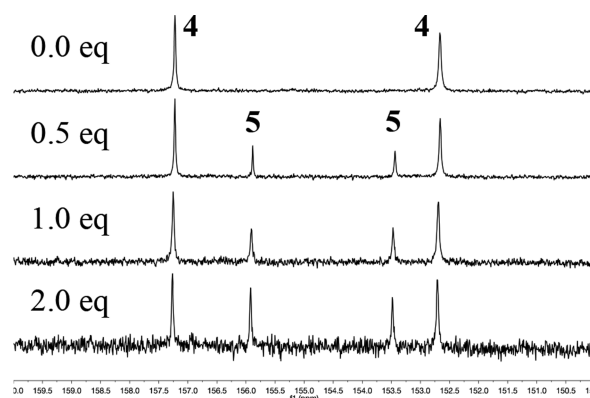


Figure 8. Partial ^{13}C NMR spectra of 0.20 M enolate **2** and 1.0 M TMEDA with various equivalents of excess NaDA (as indicated) in toluene at -80°C . Monomer **4** and mixed dimer **5** are shown.

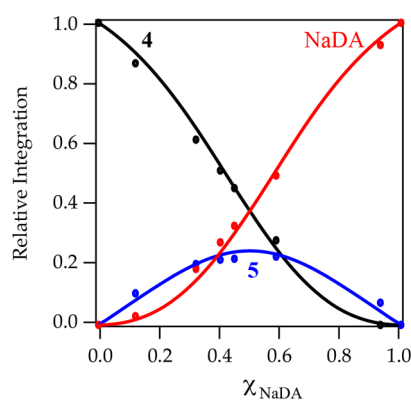
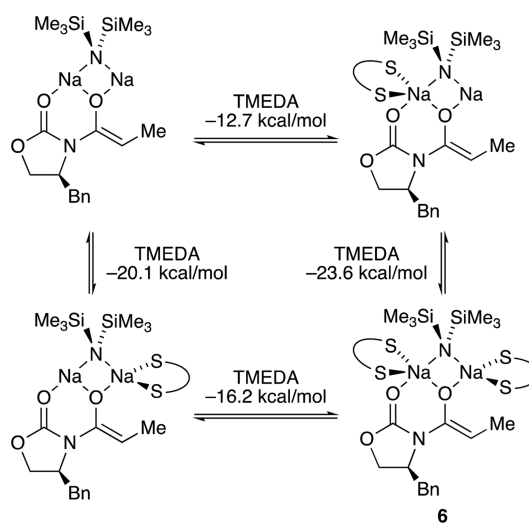


Figure 9. Job plot showing the relative integrations of NaDA (red), enolate monomer **4** (black), and mixed dimer **5** (blue) versus the measured mole fraction of NaDA with various proportions of NaDA and enolate (0.40 M total sodium titer) in 1.0 M TMEDA/toluene at -80°C . The ratios were ascertained by following the resonances of monomer **4** (carbonyl carbon at $\delta 157.3$), mixed dimer **5** (carbonyl carbon at $\delta 155.5$ and NaDA methyne carbon at $\delta 50.4$), and NaDA (NaDA methyne carbon $\delta 50.2$ ppm).

Scheme 1. Serial Solvation of NaHMDS To Give Mixed Dimer **6**



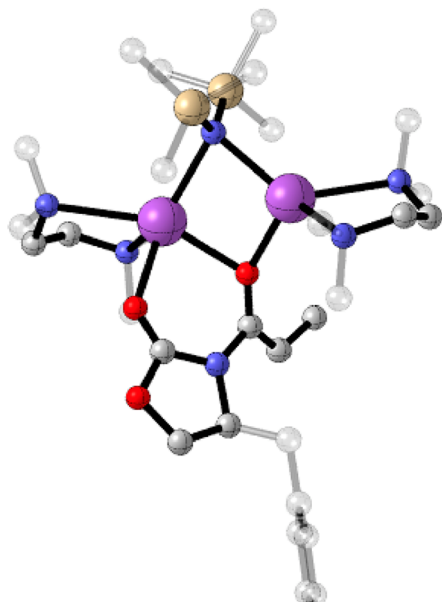
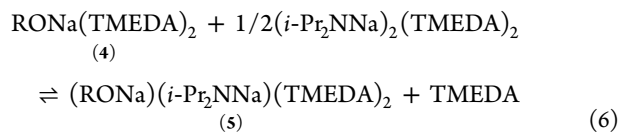


Figure 10. Computed structure of bis-TMEDA-chelated mixed dimer 6.

Structures of Enolate–Phenolate Mixed Dimers.

Hoping to exploit mixed dimers to control the selectivity of enolate functionalizations (*vide infra*), we found that insoluble sodium 2,6-di-*tert*-butylphenolate²⁷ suspended in TMEDA/toluene is solubilized by enolate 2 to form mixed dimer 7 quantitatively (Figure 11). The 1:1 enolate–phenolate stoichiometry was shown with ¹³C NMR spectroscopy. Although ligand exchange was too fast for the direct measurement of the number of coordinated TMEDA ligands, DFT computations showed exothermic double chelation and support the structure in Figure 12. The phenolate moiety shows a significant cant away from the oxazolidinone for

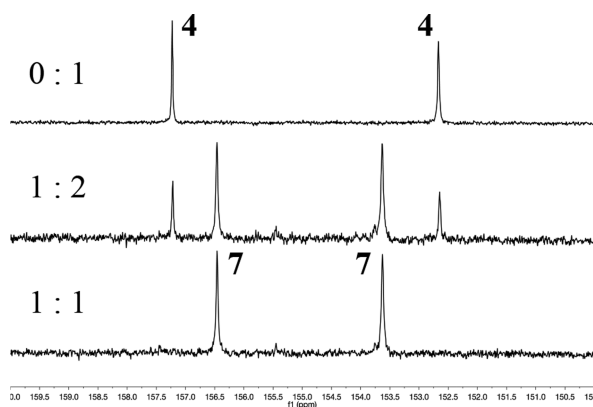


Figure 11. ¹³C NMR spectra of mixtures containing enolate 2 and sodium 2,6-di-*tert*-butylphenolate (0.30 M total sodium titer) in 1.0 M TMEDA/toluene at $-80\text{ }^{\circ}\text{C}$ showing monomer 4 and mixed aggregate 7. The concentrations of phenolate are 0.00, 0.10, and 0.15 (1.0 equiv), respectively.

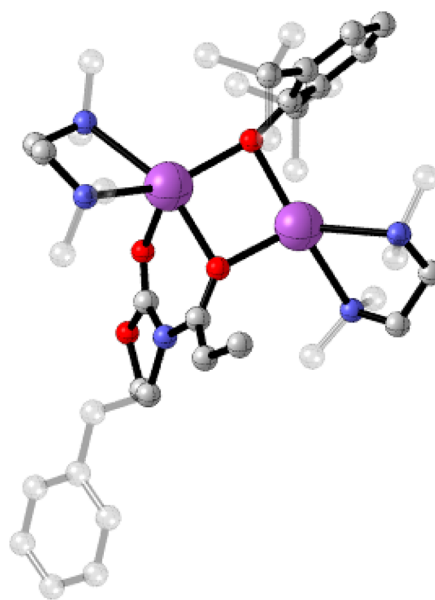


Figure 12. Computed structure of sodium 2,6-di-*tert*-butylphenolate-containing mixed dimer 7 solvated by TMEDA.

reasons that are not obvious. The approximate planes defined by the Na_2O_2 and oxazolidinone rings are skewed by $>60^{\circ}$.

Kinetics of Alkylation.²⁸ Technical problems with using in situ IR spectroscopy to study the allylation of monomer 4 (generic enolate 2 in eq 1) prompted us to monitor the loss of allyl bromide with ¹H NMR spectroscopy. Pseudo-first-order conditions were established by maintaining standard concentrations of enolate 4 (0.050–0.50 M) and 2.0 equiv TMEDA per sodium (0.10–1.0 M) with low allyl bromide concentrations (0.010 M), all in toluene. The loss of allyl bromide follows a clean pseudo-first-order decay (Figure 13). Following

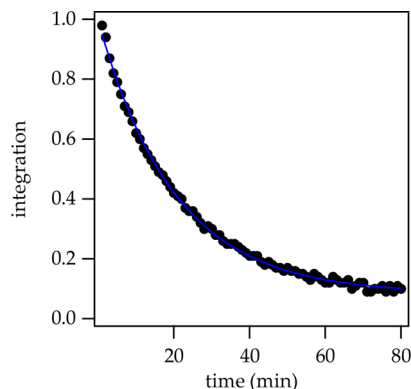


Figure 13. Plot following the loss of allyl bromide (0.010 M) by enolate monomer 4 (0.40 M) in 1.0 M TMEDA/toluene at $-20\text{ }^{\circ}\text{C}$. The curve depicts a least-squares fit to $y = ae^{-bx}$, such that $b = k_{\text{obsd}}$.

an alkylation to full consumption of enolate shows no evidence of autoinhibition or autocatalysis. The other dependencies were determined using the method of initial rates.²⁹ Plotting initial rates versus enolate and TMEDA concentration revealed first and zeroth orders, respectively (Figures 14 and 15). The rate data are consistent with the idealized³⁰ rate law in eq 7 and the generic mechanism in eq 8. DFT computations suggest a massive 2000:1 preference at $-20\text{ }^{\circ}\text{C}$ (3.9 kcal/mol; eq 1) compared with the more modest 20:1 diastereoselectivity

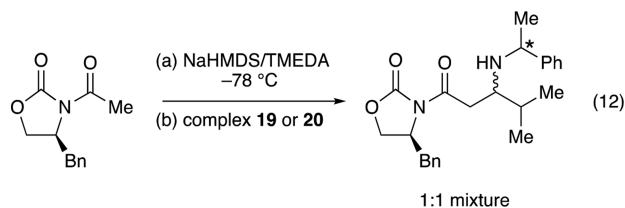
Table 1. Selectivities for Quaternization of Oxazolidinone 13 (eq 10)

Entry	Solvent	Yield (%)	14 (S/R)
1	THF	Decomp	
2	TMEDA	54	11:1
3	DME	40	11:1
4	Et ₃ N	70	11:1
5	Et ₃ N then (R,R)-TMCDA	71	11:1
6	(R,R)-TMCDA	40	30:1
7	(S,S)-TMCDA	52	19:1
8	7/TMEDA	44	11:1

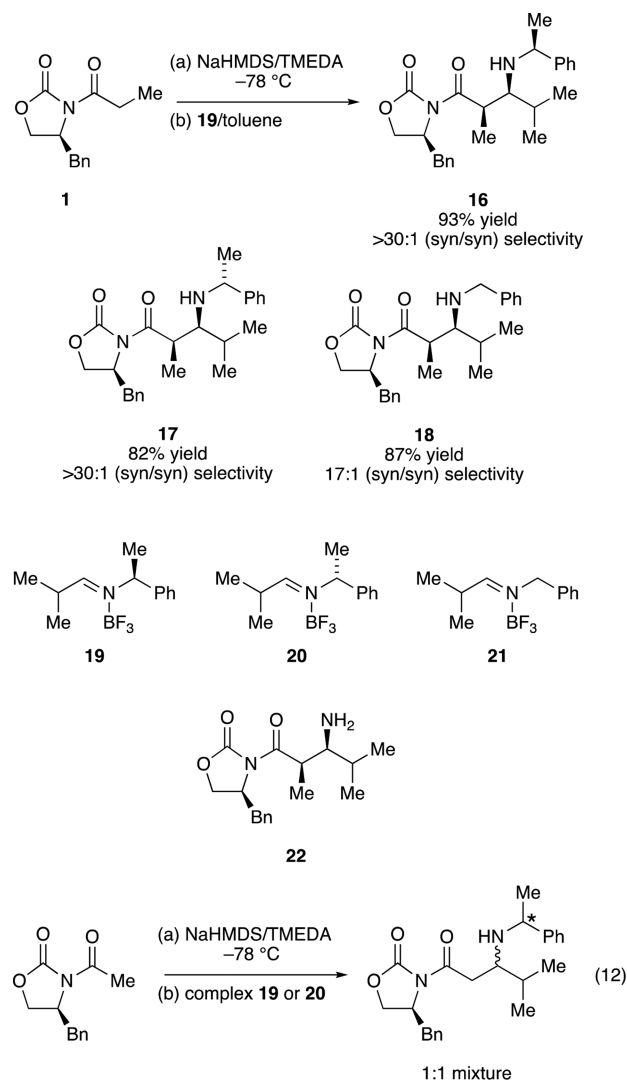
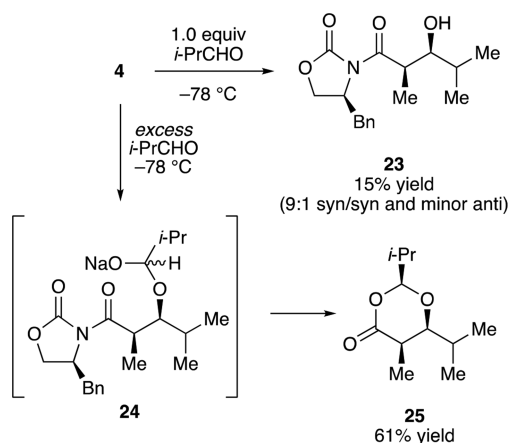
poorly solvating conditions, precomplexation of the substrate was observable with IR.³⁵ Enolization using NaHMDS/Et₃N/toluene with *subsequent* addition of (R,R)-TMCDA gave identical results (entry 5). The isolated yields roughly correlate with the suppression of the deacylation. NaHMDS/(R,R)-TMCDA afforded improved selectivities (30:1) with a sacrificed yield (40%; entry 6), whereas NaHMDS/(S,S)-TMCDA gave 19:1 selectivity in 52% yield (entry 7). Adding di-*tert*-butylphenolate (possibly forming an analog of mixed dimer 7) gave the standard 11:1 selectivity in 44% yield (entry 8).

Azaaldol Additions. A brief examination of other electrophiles afforded nothing of interest with epoxides even with assistance from BF₃.³⁶ The azaaldol addition, however, proved productive. Simple imines are too unreactive to compete with enolate decomposition. Noting success using imines activated with strongly electron withdrawing substituents,^{37–40} we turned to highly reactive BF₃–imine complexes⁴¹ while adding the phenethyl moiety, hoping to amplify the stereocontrol (Scheme 2).³⁹

The addition of BF₃–imine complex **19** dissolved in toluene to enolate **2** in TMEDA/toluene at –78 °C afforded adduct **16** in >30:1 selectivity and 93% yield. Adding BF₃–Et₂O to an imine/enolate mixture was considerably less effective. The antipodal BF₃–imine complex **20** afforded **17** in an analogously high (>30:1) selectivity and 82% yield. Hydrogenolyses of **16** and **17** both afforded adduct **22**.⁴² Thus, contrary to some 1,2-additions to phenethyl imines showing high stereochemical control,^{40,43} the stereochemistry of the phenethylimine moiety had no effect whatsoever. Benzylimine–BF₃ complex **21** afforded adduct **18** in 17:1 stereoselectivity and 87% yield. The steric demands of the phenethyl moiety may have some consequence. We hoped that even acetate-based azaaldols would be selective, but no stereocontrol was observed (eq 12).



Aldol Additions. Aldol addition to 1.0 equiv *i*-PrCHO afforded a low yield of aldol **23** owing to the formation of acetal **25** with credible stereocontrol (Scheme 3). Aldol addition in the presence of excess *i*-PrCHO afforded acetal **25** contaminated with approximately 10% total of three minor diastereomers in a nonoptimized 61% isolated yield. Acetal **25**

Scheme 2. 1,2-Additions of Enolate 2 to Imine–BF₃ Complexes**Scheme 3. Aldol Addition and Aldehyde-Mediated Deacylation**

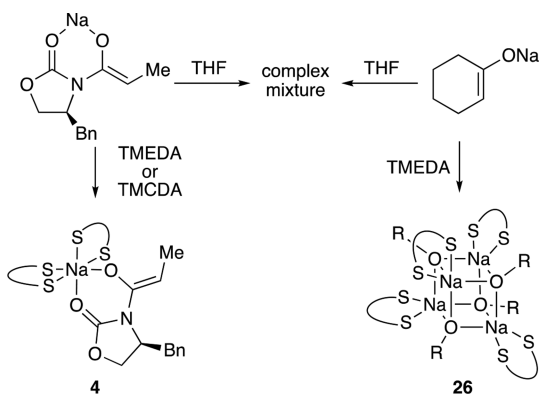
presumably forms via 1,2-adduct **24**. Treating stereochemically pure syn aldol adduct **23** sequentially with 1.0 equiv of NaHMDS (to generate the alkoxide) and *i*-PrCHO afforded **25** in an unoptimized 59% yield with no loss of syn

stereoselectivity. Acetal **25** from the aldol addition-cyclization sequence was shown to be an 7:1 mixture of enantiomers reflecting the original syn:syn selectivity.⁴⁴

DISCUSSION

Structures of TMEDA-Solvated Enolates. Our fledgling studies of sodiated enolates have produced decidedly different results than studies of their lithium counterparts (Scheme 4).¹²

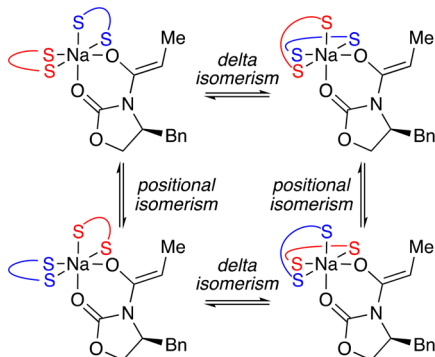
Scheme 4. Structures of Sodium Enolates in THF and TMEDA/Toluene



For example, lithium cyclohexenolate is tetrameric in THF and a doubly chelated dimer in TMEDA/toluene.⁴⁵ By contrast, sodium cyclohexenolate is intractably complex in THF and forms chelated tetramer **26** in TMEDA/toluene.¹¹ Similar bifurcated behavior is observed with Evans enolates. Lithiated Evans enolates are predominantly unsolvated tetramers in either TMEDA or THF.⁵ The sodium analogs are, once again, spectroscopically intractable in THF yet exclusively chelated monomers (**4**) in TMEDA/toluene.

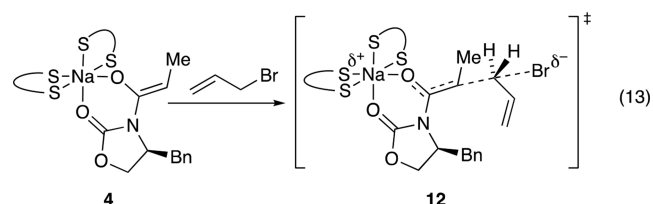
The *two* chelating diamines in **4** cause highly characteristic mixed solvates in binary mixtures of TMEDA, (*R,R*)-TMEDA, and (*S,S*)-TMEDA. The details were obscured by broadened resonances and limited resolution that attest to the stereochemical complexity presented by the octahedral environment of **4** (Scheme 5). If the chelated diamines in **4** (depicted using red and blue color coding) are both TMEDA, there are two delta isomers⁴⁶ suggested by DFT computations to have nearly equal energy (0.4 kcal/mol; see Figure 5). Each delta isomer contains two magnetically inequivalent TMEDA ligands manifesting eight magnetically inequivalent methyls—16 in

Scheme 5. Positional and Delta Isomers of Octahedral Monomeric Enolates



total. In the limit of slow conformational exchange of TMEDA—half-chair conformers that are well-documented for TMEDA—lithium chelates⁴⁷—would cause that number to spike. The stereochemical complexity doubles with mixtures of structurally distinct diamines (denoted as red and blue in Scheme 5) when delta isomerism and *positional* isomerism are superimposed. DFT computations predict the four isomers in Scheme 5 to be within <1.0 kcal/mol for the (*S,S*)-TMEDA/TMEDA mixed solvate, for example. Thus, we were *never* going to resolve all the magnetically inequivalent resonances and consider it fortunate that we could detect and measure the total populations of the mixed and homosolvates by focusing on the enolate sp^2 carbons.

Mechanism and Stereochemistry of Alkylation. The mechanism of alkylation of monomer **4** is simple, occurring via a doubly chelated monomer (Figure 16) without any invasive structural changes. DFT computations markedly overestimate the observed 20:1 selectivity but are qualitatively consistent (eq 13). The simplicity of an observable monomer reacting as

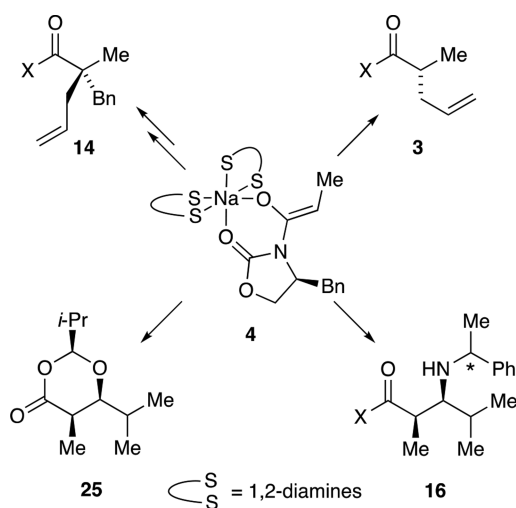


monomer contrasts with the reaction of lithium Evans enolates in THF solution, in which a kinetically generated mixture of isomeric dimers readily ages to predominantly tetramer, and with the reaction of sodium enolate **2** in THF, which seems to exist as an ill-defined but obviously quite complex mixture of species. Owing to pre-equilibria, explicit correlations of observable structure with reactivity and selectivity are questionable. Nonetheless, years of experience have shown that high stereocontrol is often accompanied by good structural control. For the allylation in eq 1, we observed no advantages or disadvantages offered by TMEDA/toluene compared with THF, but that is not universally the case (*vide infra*).

Enolate Quaternization. There are relatively few quaternizations of Evans enolates, and they tend to be specialized cases such as those bearing sterically undemanding α -fluoro or α -alkoxy moieties.^{31,48} In our hands, the quaternization (Scheme 6 and eq 10) completely fails in THF solution owing to competitive deacylation. By contrast, TMEDA-solvated enolate—presumably a bis-chelated monomer analogous to **4**—gave 54% yield and 11:1 diastereoselectivity. The stereochemistry appeared to be dictated by a fully equilibrated *Z/E* enolate mixture. There are potentially superior protocols,³¹ but quaternizations of TMEDA-solvated Evans enolates may find a niche and certainly underscore a uniqueness of monomeric enolate **4**.

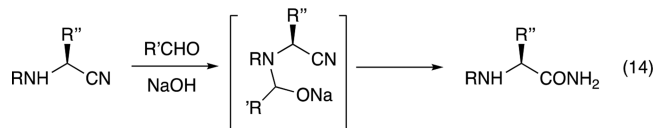
Other Electrophiles. A casual survey of electrophiles showed that TMEDA-solvated monomer **4** might find broader applications (Scheme 6). The most notable results come from additions of **4** to preformed imine- BF_3 complexes. 1,2-Additions of Evans enolates to activated imines are rare.³⁸ Although the addition formed adduct **16** in good yield with essentially total stereoselectivity (>30:1), the choice of phenethylimine antipode had no influence on the selectivity whatsoever; the oxazolidinone auxiliary was the dominant

Scheme 6. Reactions of Diamine-Solvated Monomeric Enolate 4



control element. Equally surprising on the other end of the scale, an acetate-based addition was totally unselective irrespective of the phenethylimine antipode.

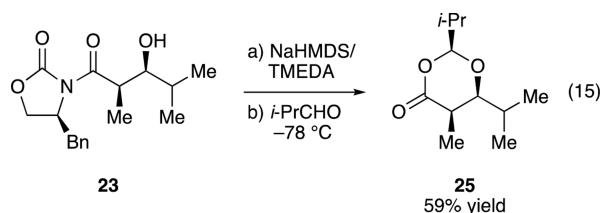
We suspect that relatively few attempts have been made to exploit sodiated Evans enolates for aldol additions; we found one report.⁴⁹ This is to be expected given the limited attention received by their lithium counterparts.⁷ Indeed, we observed low yields of addition to *i*-PrCHO, albeit with a credible stereoselectivity (Scheme 3). The major byproduct was acetal 25, presumably formed via 1,2-adduct 24. Using excess *i*-PrCHO affords acetal 25 in 61% yield (Scheme 3). We suspect that the diastereoselective cyclization required to control the stereochemistry at the acetal-based stereogenic center arises from reversible adduct formation and selective closure. Adduct 24 is reminiscent of the compounds exploited by Beauchemin and co-workers using aldehydes as organocatalysts (eq 14),⁵⁰



as well as the key intermediates in a tandem aldol addition and Tishchenko reaction.⁵¹ We have previously suggested that transiently and reversibly formed 1,2-adducts may be prevalent but undetected.⁶

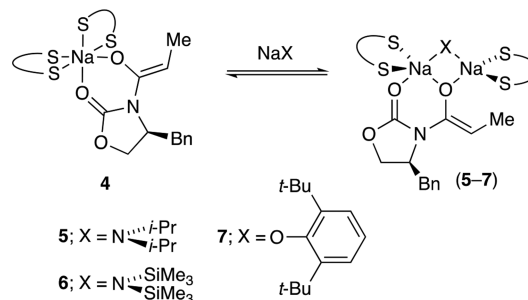
The formation of 25 poses a number of synthetically notable possibilities. Precluding the retroaldol may be the source of the markedly increased yield relative to that of the simple aldol addition. A potentially four-pot sequence—aldol addition, alcohol protection, deacylation, and esterification—is telescoped to one in >90% yield per step. The premature removal of the auxiliary, however, causes the stereochemical refinement of adducts analogous to 23 to become a problem of refining optical purity. In the spirit of Beauchemin's results, stereochemically pure *syn* aldol adduct 23 can be transformed to 25 in a single step with an unoptimized 59% yield and no loss of diastereoselectivity (eq 15). This one-step replacement of what would otherwise be a three-step protocol may have some synthetic utility in polyketide synthesis.

Mixed Aggregate Structure and Reactivity. Admittedly limited studies to date have shown little evidence of mixed



aggregation in NaDA/NaX mixtures,^{52,53} which is quite unlike the often-observed LDA–LiX mixed aggregates.²⁵ We were surprised, therefore, to observe sodium enolate–sodium amide mixed dimers 5 and 6 (Scheme 7). Moreover, NaHMDS forms

Scheme 7. Mixed Aggregation with Evans Enolates



mixed dimer 6 quantitatively, whereas the analogous NaDA–sodium enolate mixed dimer 5 is formed in a much softer (nonquantitative) equilibrium. The reverse is true for LiHMDS and LDA.²⁵ Even insoluble sodium di-*tert*-butylphenolate is drawn into solution to form mixed dimer 7 quantitatively.

Mixed aggregates 5–7 could impose stereochemical control over the alkylations provided that the mixed aggregates react without dissociation to monomer 4.^{54,55} Although alkylations of 5 and 6 gave poor results presumably owing to the nefarious reactivities of the sodium amide fragments, the phenolate-derived mixed dimer 7 showed promise: it reacted cleanly and altered the product distribution, albeit in the wrong direction (eq 9). Here is why we still find the experiment interesting. If mixed dimer 7 reacts directly without invasive structural changes, there is a stereocontrol element that is unavailable to monomer 4 (Figure 17). The monomer has a sodium and

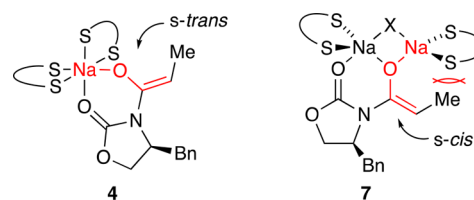


Figure 17. Illustration of *s-cis* and *s-trans* alignments.

affiliated ligands in an *s-trans* orientation relative to the enolate carbon, placing potential stereochemically controlling ligands remote from the nucleophilic enolate carbon. By contrast, the dimer has an *s-cis* orientation. Despite early failures to improve the selectivity, we sense that persistence in the choice of salt (NaX) and diamine could lead to success.

CONCLUSION

Sodiated Evans enolates are often used for stereoselective alkylations; however, they are *not* just “lithium enolates on steroids”. TMEDA-solvated monomer **4** has good structural control compared with the analogous enolate in THF solution and offers comparable alkylation selectivities and yields, allows for quaternizations, and exhibits potentially useful reactivities toward imines and aldehydes.

The contrasting behavior of THF and TMEDA raises an important issue. The development of organometallic chemistry is a story of ligand development and optimization. Whether we are speaking of transition-metal-catalyzed couplings or organolithium-based metalations, the coordination sphere is paramount. The temptation to use THF for sodium chemistry because it works so well for lithium may be misguided. Organolithium reagents dominate organoalkali metal chemistry despite lower reactivities because of their higher selectivities. We are not convinced that this will necessarily be the case going forward. Achieving high selectivities in organosodium chemistry may stem from the development of ligands for the larger sodium ion.

EXPERIMENTAL SECTION

Reagents and Solvents. THF, TMEDA, TMCDA, and toluene were distilled from solutions containing sodium benzophenone ketyl. NaDA¹⁴ and NaHMDS were prepared and purified as described previously.¹⁶ Oxazolidinones are commercially available or prepared according to literature procedures.⁵⁶ Air- and moisture-sensitive materials were manipulated under argon with standard glovebox, vacuum line, and syringe techniques.

IR Spectroscopic Analyses. IR spectra were recorded with an *in situ* IR spectrometer fitted with a 30-bounce, silicon-tipped probe. The spectra were acquired in 16 scans at a gain of 1 and a resolution of 4 cm⁻¹. A representative reaction was carried out as follows: The IR probe was inserted through a nylon adapter and O-ring seal into an oven-dried, cylindrical flask fitted with a magnetic stir bar and a T-joint. The T-joint was capped with a septum for injections and a nitrogen line. After evacuation under full vacuum, heating, and flushing with nitrogen, the flask was charged with NaHMDS (101 mg, 0.55 mmol) in 1.0 M TMEDA/toluene and cooled to -78 °C. After recording a background spectrum, oxazolidinone **1** (116.5 mg, 0.50 mmol) in toluene was added. The absorbance of **1** at 1783 cm⁻¹ was immediately replaced with an absorbance of enolate **2** at 1743 cm⁻¹. To this solution was added neat allyl bromide (363 mg, 3.0 mmol), causing the enolate absorbance to be replaced by the absorbance of oxazolidinone **3** (1783 cm⁻¹). IR spectra were recorded every 15 s with monitoring of the absorbance at 1783 cm⁻¹ over the course of the reaction.

NMR Spectroscopy. Individual stock solutions of substrates and NaHMDS were prepared at room temperature. An NMR tube under vacuum was flame-dried on a Schlenk line, allowed to cool to room temperature, backfilled with argon, and placed in a -78 °C dry ice/acetone bath. Appropriate amounts of oxazolidinone and NaHMDS (1.1 equiv) were added sequentially via syringe. The tube was sealed under partial vacuum and vortexed three times on a vortex mixer for 5 s with cooling between each vortexing. Samples could be stored overnight in a -86 °C freezer. Standard ¹H and ¹³C NMR spectra were recorded on a 500 MHz spectrometer at 500 and 125.79 MHz, respectively. The ¹H and ¹³C resonances are referenced to CDCl₃ (7.26 and 77.16 ppm, respectively) and toluene-*d*₈ (C₆D₅CD₃ at 20.4 ppm).

NMR Reaction Kinetics. An NMR tube was charged with reagents as described above. The sample was vortexed three times on a vortex mixer for 5 s with cooling between each vortexing. To this solution, allyl bromide was added. The reaction was followed by ¹H NMR spectroscopy at -20 °C recording spectra at 1.0 min intervals.

Preparation of 3. To a solution of NaHMDS (0.60 mmol, 110 mg) and TMEDA (1.2 mmol, 180 μL) in 4.5 mL of toluene under argon at -78 °C was added **1** (0.50 mmol, 116.5 mg) in 0.50 mL of toluene. After stirring for 30 min, allyl bromide (3.0 mmol, 260 μL) was injected, and the vessel was warmed to 0 °C. The reaction was quenched by 5.0 mL of saturated NH₄Cl and extracted three times with EtOAc. The organic extracts were dried over MgSO₄ and concentrated in vacuo. Flash chromatography with 20% ethyl acetate in hexanes provided 132 mg (97% yield) shown by ¹H NMR spectroscopy to be a 20:1 diastereomeric mixture of **3** and its isomer analogous to that reported previously.³³

Preparation of 13. To a solution of NaHMDS (3.3 mmol, 605 mg) and TMEDA (6.6 mmol, 988 μL) in 5.0 mL of toluene under argon at -78 °C was added **1** (3.0 mmol, 699 mg) in 1.0 mL of toluene. The reaction was stirred for 30 min, charged with benzyl bromide (20 mmol, 2.4 mL), warmed to 0 °C, and stirred for 0.5 h. The reaction was quenched with 5.0 mL of saturated NH₄Cl and extracted three times with EtOAc. The organic extracts were dried over MgSO₄ and concentrated in vacuo. Flash chromatography with 20% ethyl acetate in hexanes afforded 825 mg of **13** (85% combined yield) displaying spectroscopic properties described previously.³³

Preparation of 14. To a solution of NaHMDS (0.10 mmol, 18.3 mg) and TMEDA (0.20 mmol, 30 μL) in toluene (2.0 mL) under argon was added **13** (0.070 mmol, 22.6 mg) in 0.10 mL of toluene. The reaction mixture was stirred under argon for 1 h at -20 °C. Allyl bromide (0.40 mmol, 35 μL) was injected, and the mixture was warmed to 0 °C over 2 h. The reaction was quenched with 3.0 mL of saturated NH₄Cl and extracted three times with EtOAc. The organic extracts were dried over MgSO₄ and concentrated in vacuo. Flash chromatography with 15% ethyl acetate in hexanes afforded 13.7 mg of product (54% combined yield) shown to be an 11:1 mixture of **14** and its minor diastereomer. ¹H NMR (599 MHz, CDCl₃) δ 7.34–7.30 (m, 2H), 7.28–7.24 (m, 3H), 7.23–7.19 (m, 5H), 5.77 (dddd, *J* = 16.9, 10.1, 8.0, 6.7 Hz, 1H), 5.11 (dq, *J* = 17.0, 1.6 Hz, 1H), 5.06 (ddt, *J* = 10.0, 2.0, 1.0 Hz, 1H), 4.61 (ddt, *J* = 10.7, 6.7, 3.3 Hz, 1H), 4.15–4.10 (m, 2H), 3.61 (d, *J* = 13.6 Hz, 1H), 3.18 (dd, *J* = 13.2, 3.3 Hz, 1H), 3.12–3.04 (m, 2H), 2.61 (dd, *J* = 13.2, 10.6 Hz, 1H), 2.29 (ddt, *J* = 14.3, 6.7, 1.4 Hz, 1H), 1.36 (s, 3H). ¹³C NMR (126 MHz, CDCl₃) δ 176.07, 152.77, 137.72, 135.94, 134.39, 130.58, 129.54, 129.06, 128.20, 127.38, 126.74, 118.27, 66.43, 58.32, 50.54, 42.01, 40.73, 38.01, 23.38. *m/z* calculated for (M+H)⁺ 364.19072, found 364.19097.

Confirming the Structure of 14. To a solution of **14** (0.050 mmol, 18 mg) in THF (0.45 mL) and water (0.15 mL) at 0 °C was added H₂O₂ (30%, 40 mL) dropwise and LiOH (2.4 mg) in water (0.10 mL). The reaction was warmed to 20 °C for 2 h, cooled to 0 °C, and treated with Na₂SO₃ (56.8 mg) in water (0.3 mL) with stirring at 20 °C for 12 h. The reaction was concentrated in vacuo, and its pH was adjusted to 13 using NaOH at 0 °C. The aqueous solution was extracted three times with CH₂Cl₂, and pH was brought to 1 using concentrated HCl at 0 °C. The mixture was extracted three times with EtOAc, dried over MgSO₄, and concentrated in vacuo to afford 7 mg of product (69% combined yield). ¹H NMR (500 MHz, CDCl₃) δ 7.30–7.21 (m, 3H), 7.20–7.14 (m, 2H), 5.82 (ddt, *J* = 18.5, 9.2, 7.4 Hz, 1H), 5.17–5.09 (m, 2H), 3.05 (d, *J* = 13.4 Hz, 1H), 2.78 (d, *J* = 13.4 Hz, 1H), 2.53 (ddt, *J* = 13.8, 6.9, 1.3 Hz, 1H), 2.21 (ddt, *J* = 13.7, 7.7, 1.2 Hz, 1H), 1.12 (s, 3H). ¹³C NMR (126 MHz, CDCl₃) δ 183.05, 137.33, 133.75, 130.35, 128.23, 126.77, 118.76, 47.48, 44.89, 43.33, 20.72. *m/z* calculated for (M+H)⁺ 205.12231, found 205.12198. [α]²² = +12, *c* 0.35, DCM. An authentic sample was prepared using the procedure of Myers and co-workers.⁵⁷ [α]²² = +24, *c* 0.5, CH₂Cl₂.

Preparation of Imine Adduct 16. To a solution of NaHMDS (1.0 mmol, 183 mg) and TMEDA (2.0 mmol, 300 μL) in toluene (4.5 mL) was added **1** (1.0 mmol, 233 mg) followed by stirring under argon for 30 min at -78 °C. A solution of imine-BF₃ complex **19** (1.0 mmol) in toluene (0.20 mL) was injected. After stirring for 30 min, the reaction was quenched by 5.0 mL saturated NH₄Cl and extracted three times with EtOAc. The organic extracts were dried over MgSO₄ and concentrated in vacuo. The crude product was analyzed with ¹H

NMR showing **16** in >30:1 selectivity. Flash chromatography (10% ethyl acetate/hexanes/3% Et₃N) afforded **16** (380 mg, 93% yield). ¹H NMR (500 MHz, CDCl₃) δ 7.33 (dt, *J* = 7.6, 2.8 Hz, 4H), 7.31–7.25 (m, 3H), 7.25–7.19 (m, 3H), 4.70 (ddt, *J* = 10.9, 7.2, 3.4 Hz, 1H), 4.20–4.15 (m, 1H), 4.15–4.11 (m, 1H), 3.95 (p, *J* = 6.8 Hz, 1H), 3.86 (q, *J* = 6.5 Hz, 1H), 3.40 (dd, *J* = 13.2, 3.4 Hz, 1H), 2.88 (dd, *J* = 6.2, 4.8 Hz, 1H), 2.60 (dd, *J* = 13.1, 10.4 Hz, 1H), 1.67 (pd, *J* = 6.9, 4.9 Hz, 1H), 1.33 (d, *J* = 6.6 Hz, 3H), 1.29 (d, *J* = 6.9 Hz, 3H), 0.80 (d, *J* = 6.8 Hz, 6H). ¹³C NMR (126 MHz, CDCl₃) δ 177.35, 153.32, 146.49, 135.64, 129.48, 129.13, 128.37, 127.46, 127.27, 127.02, 66.17, 61.44, 57.74, 55.71, 41.64, 38.38, 32.49, 24.25, 20.74, 17.86, 13.82. *m/z* calculated for (M+H)⁺ 409.24857, found 409.24889.

Preparation of Imine Adduct 17. Adduct **17** was prepared as described for adduct **16** using imine–BF₃ complex **20**. ¹H NMR spectroscopy of the crude shows **17** in >30:1 selectivity. Flash chromatography (10% ethyl acetate/hexanes/3% Et₃N) afforded **17** in 82% yield. ¹H NMR (500 MHz, CDCl₃) δ 7.37–7.30 (m, 4H), 7.30–7.24 (m, 3H), 7.22–7.16 (m, 3H), 4.63 (ddt, *J* = 10.8, 7.3, 3.4 Hz, 1H), 4.16–4.10 (m, 1H), 4.09 (dd, *J* = 9.1, 3.4 Hz, 1H), 3.96–3.86 (m, 2H), 3.25 (dd, *J* = 13.2, 3.4 Hz, 1H), 2.87 (dd, *J* = 6.7, 4.2 Hz, 1H), 2.52 (dd, *J* = 13.2, 10.3 Hz, 1H), 1.80 (pd, *J* = 6.9, 4.2 Hz, 1H), 1.34 (d, *J* = 6.5 Hz, 3H), 1.12 (d, *J* = 6.9 Hz, 3H), 1.07 (d, *J* = 6.9 Hz, 3H), 0.96 (d, *J* = 6.9 Hz, 3H). ¹³C NMR (126 MHz, CDCl₃) δ 177.23, 153.22, 146.33, 135.63, 129.48, 129.09, 128.42, 127.43, 127.16, 127.00, 66.04, 60.80, 56.84, 55.53, 40.84, 38.16, 31.84, 24.32, 20.67, 18.09, 14.15. *m/z* calculated for (M+H)⁺ 409.24857, found 409.24796.

Preparation of Imine Adduct 18. Adduct **18** was prepared as described for adduct **16** using imine–BF₃ complex **21** in 87% yield. ¹H NMR spectroscopy of the crude shows **18** and its minor diastereomer in 17:1 selectivity. Flash chromatography (10% ethyl acetate/hexanes/3% Et₃N) afforded **18** (34.3 mg, 87% yield). ¹H NMR (500 MHz, CDCl₃) δ 7.39–7.34 (m, 2H), 7.34–7.30 (m, 2H), 7.30–7.24 (m, 3H), 7.24–7.21 (m, 3H), 4.73 (ddt, *J* = 11.0, 7.3, 3.5 Hz, 1H), 4.20–4.15 (m, 1H), 4.14 (dd, *J* = 9.1, 3.6 Hz, 1H), 4.06–3.99 (m, 1H), 3.86 (d, *J* = 12.5 Hz, 1H), 3.81 (d, *J* = 12.5 Hz, 1H), 3.40 (dd, *J* = 13.2, 3.4 Hz, 1H), 2.90 (t, *J* = 6.0 Hz, 1H), 2.60 (dd, *J* = 13.1, 10.4 Hz, 1H), 1.81 (pd, *J* = 13.3, 6.7 Hz, 1H), 1.25 (d, *J* = 6.9 Hz, 3H), 1.04 (d, *J* = 6.8 Hz, 3H), 1.03 (d, *J* = 6.8 Hz, 3H). ¹³C NMR (126 MHz, CDCl₃) δ 176.99, 153.30, 141.05, 135.60, 129.43, 129.09, 128.46, 128.28, 127.42, 127.06, 66.20, 64.67, 55.57, 55.30, 41.14, 38.33, 32.33, 20.42, 18.83, 12.57. *m/z* calculated for (M+H)⁺ 395.23292, found 395.23215.

Hydrogenolysis. To a solution of **17** (0.08 mmol, 33.3 mg) in methanol (2 mL) was added palladium on carbon (0.008 mmol, 8.5 mg). The reaction mixture was stirred under 1.0 atm of H₂ for 24 h at room temperature. After filtering through Celite and concentrating in vacuo, flash chromatography with 3% triethylamine in ethyl acetate afforded **22** (14.5 mg, 60% yield). Peak broadening presumably owing to hydrogen bonding was mitigated by warming to 60 °C. ¹H NMR (599 MHz, CDCl₃, 60 °C) δ 7.26–7.25 (m, 1H), 7.25–7.20 (m, 3H), 7.20–7.16 (m, 1H), 5.17–5.05 (m, 2H), 4.02–3.95 (m, 1H), 3.83 (dd, *J* = 12.0, 3.0 Hz, 1H), 3.24 (dd, *J* = 13.7, 9.7 Hz, 1H), 3.12 (dd, *J* = 13.7, 6.9 Hz, 1H), 2.66 (p, *J* = 7.0 Hz, 1H), 1.64 (pd, *J* = 14.0, 6.9 Hz, 1H), 0.97–0.87 (m, 3H), 0.86 (d, *J* = 6.7 Hz, 3H), 0.83 (d, *J* = 6.6 Hz, 3H). ¹³C NMR (126 MHz, CDCl₃) δ 171.32, 155.43, 138.18, 129.51, 128.49, 126.62, 63.85, 60.55, 55.92, 34.67, 27.90, 18.77, 18.18, 14.35, 9.89. *m/z* calculated for (M+H)⁺ 305.18597, found 305.18521.

Aldol Addition. To a solution of NaHMDS (0.3 mmol, 54.9 mg) and TMEDA (0.9 mmol, 144 μL) in toluene (3 mL) was added **1** (0.3 mmol, 69.9 mg) in 0.10 mL of toluene. After stirring under argon for 30 min at –78 °C isobutyraldehyde (0.9 mmol, 82 μL) was injected and the mixture was stirred for 1 h at –78 °C. After quenching with 1.0 mL saturated NH₄Cl and extracting three times with EtOAc, the organic extracts were dried over MgSO₄ and concentrated in vacuo. Flash chromatography with 10% ethyl acetate in hexanes afforded 36.4 mg of **25** (61% combined yield). ¹H NMR showed a 17:1:0.7:0.4 mixture of **25** and three minor stereoisomers. ¹H NMR (599 MHz, CDCl₃) δ 5.06 (d, *J* = 4.2 Hz, 1H), 3.39 (dd, *J* = 9.0, 3.7 Hz, 1H), 2.73 (qd, *J* = 7.2, 3.7 Hz, 1H), 1.98 (hd, *J* = 6.9, 4.2 Hz, 1H), 1.84

(dh, *J* = 9.0, 6.6 Hz, 1H), 1.23 (d, *J* = 7.2 Hz, 3H), 1.01–0.97 (m, 9H), 0.86 (d, *J* = 6.8 Hz, 3H). ¹³C NMR (126 MHz, CDCl₃) δ 172.94, 106.45, 82.07, 38.20, 32.71, 28.45, 18.67, 17.60, 16.17, 15.83, 11.74. *m/z* calculated for (M+H)⁺ 201.14852, found 201.14824.

■ ASSOCIATED CONTENT

📄 Supporting Information

The Supporting Information is available free of charge on the ACS Publications website at DOI: 10.1021/jacs.8b10364.

Spectroscopic, kinetic, and computational data (PDF)

■ AUTHOR INFORMATION

Corresponding Author

*dbc6@cornell.edu

ORCID

Zirong Zhang: 0000-0002-6720-4644

David B. Collum: 0000-0001-6065-1655

Notes

The authors declare no competing financial interest.

■ ACKNOWLEDGMENTS

We thank the National Institutes of Health (GM077167) for support.

■ REFERENCES

- (1) (a) Ager, D. J.; Prakash, I.; Schaad, D. R. 1,2-Amino Alcohols and Their Heterocyclic Derivatives as Chiral Auxiliaries in Asymmetric Synthesis. *Chem. Rev.* **1996**, *96*, 835. (b) Wu, G.; Huang, M. Organolithium Reagents in Pharmaceutical Asymmetric Processes. *Chem. Rev.* **2006**, *106*, 2596. (c) Farina, V.; Reeves, J. T.; Senanayake, C. H.; Song, J. J. Asymmetric Synthesis of Active Pharmaceutical Ingredients. *Chem. Rev.* **2006**, *106*, 2734.
- (2) Evans, D. A.; Bartroli, J.; Shih, T. L. Enantioselective Aldol Condensations. 2. Erythro-Selective Chiral Aldol Condensations via Boron Enolates. *J. Am. Chem. Soc.* **1981**, *103*, 2127.
- (3) (a) *Modern Aldol Reactions*; Mahrwald, R., Ed.; Wiley-VCH: Weinheim, 2004; Vols. 1 and 2. (b) Lin, G.-Q.; Li, Y.-M.; Chan, A. S. C. *Principles and Applications of Asymmetric Synthesis*; Wiley & Sons: New York, 2001; 135. (c) Mahrwald, R. *Aldol Reactions*; Springer: New York, 2009.
- (4) (a) Evans, D. A.; Takacs, J. M.; McGee, L. R.; Ennis, M. D.; Mathre, D. J.; Bartroli, J. Chiral enolate design. *Pure Appl. Chem.* **1981**, *53*, 1109. (b) Evans, D. A.; Ennis, M. D.; Mathre, D. J. Asymmetric Alkylation Reactions of Chiral Imide Enolates. A Practical Approach to the Enantioselective Synthesis of α -Substituted Carboxylic Acid Derivatives. *J. Am. Chem. Soc.* **1982**, *104*, 1737.
- (5) Tallmadge, E. H.; Collum, D. B. Evans Enolates: Solution Structures of Lithiated Oxazolidinone-Derived Enolates. *J. Am. Chem. Soc.* **2015**, *137*, 13087.
- (6) Tallmadge, E. H.; Jermaks, J.; Collum, D. B. Structure–Reactivity Relationships in Lithiated Evans Enolates: Influence of Aggregation and Solvation on the Stereochemistry and Mechanism of Aldol Additions. *J. Am. Chem. Soc.* **2016**, *138*, 345.
- (7) For an attempt to assemble a comprehensive bibliography of lithium-based Evans aldol additions, see ref 6.
- (8) Jermaks, J.; Tallmadge, E. H.; Keresztes, I.; Collum, D. B. Lithium Amino Alkoxide–Evans Enolate Mixed Aggregates: Aldol Addition with Matched and Mismatched Stereocontrol. *J. Am. Chem. Soc.* **2018**, *140*, 3077.
- (9) Zhang, Z.; Collum, D. B. Evans Enolates: Structures and Mechanisms Underlying the Aldol Addition of Oxazolidinone-Derived Boron Enolates. *J. Org. Chem.* **2017**, *82*, 7595.
- (10) For other examples of physical studies of Evans enolates, see: (a) Shinisha, C. B.; Sunoj, R. B. Transition State Models for Probing Stereoinduction in Evans Chiral Auxiliary-Based Asymmetric Aldol

Reactions. *J. Am. Chem. Soc.* **2010**, *132*, 12319. (b) Sreenithya, A.; Sunoj, R. B. Noninnocent Role of *N*-Methyl Pyrrolidinone in Thiazolidinethione-Promoted Asymmetric Aldol Reactions. *Org. Lett.* **2012**, *14*, 5752. (c) Shinisha, C. B.; Sunoj, R. B. The Pivotal Role of Chelation as a Stereochemical Control Element in Non-Evans Anti Aldol Product Formation. *Org. Lett.* **2010**, *12*, 2868. (d) Goodman, J. M.; Paton, R. S. Enantioselectivity in the boron aldol reactions of methyl ketones. *Chem. Commun.* **2007**, 2124. (e) Baringhaus, K. H.; Matter, H.; Kurz, M. Solution Structure of a Chiral Dialkylboron Enolate by NMR Spectroscopy and Simulated Annealing: Unusual Stabilization of This Intermediate by a Boron-Nitrogen Interaction. *J. Org. Chem.* **2000**, *65*, 5031. (f) Kimball, D. B.; Michalczyk, R.; Moody, E.; Ollivault-Shiflett, M.; De Jesus, K.; Silks, L. A., III Determining the Solution State Orientation of a Ti Enolate via Stable Isotope Labeling, NMR Spectroscopy, and Modeling Studies. *J. Am. Chem. Soc.* **2003**, *125*, 14666.

(11) Tomasevich, L. L.; Collum, D. B. Method of Continuous Variation: Characterization of Alkali Metal Enolates Using ^1H and ^{19}F NMR Spectroscopies. *J. Am. Chem. Soc.* **2014**, *136*, 9710.

(12) For an interesting historical perspective on organoalkali metal chemistry, see: (a) Seyferth, D. Alkyl and Aryl Derivatives of the Alkali Metals: Useful Synthetic Reagents as Strong Bases and Potent Nucleophiles. 1. Conversion of Organic Halides to Organoalkali-Metal Compounds. *Organometallics* **2006**, *25*, 2. (b) Seyferth, D. Alkyl and Aryl Derivatives of the Alkali Metals: Strong Bases and Reactive Nucleophiles. 2. Wilhelm Schlenk's Organoalkali-Metal Chemistry. The Metal Displacement and the Transmetalation Reactions. Metalation of Weakly Acidic Hydrocarbons. Superbases. *Organometallics* **2009**, *28*, 2.

(13) Mulvey, R. E.; Robertson, S. D. Synthetically Important Alkali-Metal Utility Amides: Lithium, Sodium, and Potassium Hexamethyldisilazides, Diisopropylamides, and Tetramethylpiperidides. *Angew. Chem., Int. Ed.* **2013**, *52*, 11470.

(14) Ma, Y.; Algera, R. F.; Collum, D. B. Sodium Diisopropylamide in *N,N*-Dimethylethylamine: Reactivity, Selectivity, and Synthetic Utility. *J. Org. Chem.* **2016**, *81*, 11312.

(15) Andrews, P. C.; Barnett, N. D. R.; Mulvey, R. E.; Clegg, W.; O'Neil, P. A.; Barr, D.; Cowton, L.; Dawson, A. J.; Wakefield, B. J. X-ray crystallographic studies and comparative reactivity studies of a sodium diisopropylamide (NDA) complex and related hindered amides. *J. Organomet. Chem.* **1996**, *518*, 85.

(16) Watson, B. T.; Lebel, H. Sodium hexamethyldisilazide. *e-EROS Encyclopedia of Reagents for Organic Synthesis*; John Wiley & Sons: New York, 2005; pp 1–10.

(17) (a) Ojeda-Amador, A. I.; Martinez-Martinez, A. J.; Kennedy, A. R.; Armstrong, D. R.; O'Hara, C. T. Monodentate coordination of the normally chelating chiral diamine (*R,R*)-TMEDA. *Chem. Commun.* **2017**, *53*, 324. (b) Henderson, K. W.; Dorigo, A. E.; Liu, Q. Y.; Williard, P. G. Effect of Polydentate Donor Molecules on Lithium Hexamethyldisilazide Aggregation: An X-ray Crystallographic and a Combination Semiempirical PM3/Single Point *ab Initio* Theoretical Study. *J. Am. Chem. Soc.* **1997**, *119*, 11855. (c) Kennedy, A. R.; Mulvey, R. E.; O'Hara, C. T.; Robertson, S. D.; Robertson, G. M. *catena*-Poly[sodium- μ_2 -(*N,N,N',N'*-tetramethylethane-1,2-diamine)- $\kappa^2\text{N}:N'$ -sodium-bis[μ_2 -bis(trimethylsilyl)azanido- $\kappa^2\text{N}:N'$]]. *Acta Crystallogr., Sect. E: Struct. Rep. Online* **2012**, *68*, m1468.

(18) *Gaussian 09*, Revision A.02, Frisch, M. J.; Trucks, G. W.; Schlegel, H. B.; Scuseria, G. E.; Robb, M. A.; Cheeseman, J. R.; Scalmani, G.; Barone, V.; Petersson, G. A.; Nakatsuji, H.; Li, X.; Caricato, M.; Marenich, A.; Bloino, J.; Janesko, B. G.; Gomperts, R.; Mennucci, B.; Hratchian, H. P.; Ortiz, J. V.; Izmaylov, A. F.; Sonnenberg, J. L.; Williams-Young, D.; Ding, F.; Lipparini, F.; Egidi, F.; Goings, J.; Peng, B.; Petrone, A.; Henderson, T.; Ranasinghe, D.; Zakrzewski, V. G.; Gao, J.; Rega, N.; Zheng, G.; Liang, W.; Hada, M.; Ehara, M.; Toyota, K.; Fukuda, R.; Hasegawa, J.; Ishida, M.; Nakajima, T.; Honda, Y.; Kitao, O.; Nakai, H.; Vreven, T.; Throssell, K.; Montgomery, J. A., Jr.; Peralta, J. E.; Ogliaro, F.; Bearpark, M.; Heyd, J. J.; Brothers, E.; Kudin, K. N.; Staroverov, V. N.; Keith, T.; Kobayashi, R.; Normand, J.; Raghavachari, K.; Rendell,

A.; Burant, J. C.; Iyengar, S. S.; Tomasi, J.; Cossi, M.; Millam, J. M.; Klene, M.; Adamo, C.; Cammi, R.; Ochterski, J. W.; Martin, R. L.; Morokuma, K.; Farkas, O.; Foresman, J. B.; Fox, D. J. *Gaussian, Inc.*; Wallingford CT, 2016.

(19) Evans, D. A.; Britton, T. C.; Ellman, J. A. Contrastive carboximide hydrolysis with lithium hydroperoxide. *Tetrahedron Lett.* **1987**, *28*, 6141.

(20) We refer to $(\text{LiX})_n$ and $(\text{LiX})_m(\text{LiX}')_n$ as a "homoaggregate" and "heteroaggregate", respectively, and reserve the term "mixed aggregate" for $(\text{LiX})_m(\text{LiY})_n$.

(21) Renny, J. S.; Tomasevich, L. L.; Tallmadge, E. H.; Collum, D. B. Method of Continuous Variations: Applications of Job Plots to the Study of Molecular Associations in Organometallic Chemistry. *Angew. Chem., Int. Ed.* **2013**, *52*, 11998.

(22) Job, P. Formation and Stability of Inorganic Complexes in Solution. *Ann. Chim.* **1928**, *9*, 113.

(23) Houghton, M. J.; Collum, D. B. Lithium Enolates Derived from Weinreb Amides: Insights into Five-Membered Chelate Rings. *J. Org. Chem.* **2016**, *81*, 11057.

(24) Hibbert, D. B.; Thordarson, P. The death of the Job plot, transparency, open science and online tools, uncertainty estimation methods and other developments in supramolecular chemistry data analysis. *Chem. Commun.* **2016**, *52*, 12792.

(25) (a) Collum, D. B. Solution Structures of Lithium Dialkylamides and Related *N*-Lithiated Species: Results from ^6Li - ^{15}N Double Labeling Experiments. *Acc. Chem. Res.* **1993**, *26*, 227. (b) Lucht, B. L.; Collum, D. B. Lithium Hexamethyldisilazide: A View of Lithium Ion Solvation Through a Glass-Bottom Boat. *Acc. Chem. Res.* **1999**, *32*, 1035.

(26) Algera, R. F.; Ma, Y.; Collum, D. B. Sodium Diisopropylamide: Aggregation, Solvation, and Stability. *J. Am. Chem. Soc.* **2017**, *139*, 7921.

(27) (a) Boyle, T. J.; Velazquez, A. T.; Yonemoto, D. T.; Alam, T. M.; Moore, C.; Rheingold, A. L. Synthesis and characterization of a family of solvated sodium aryloxide compounds. *Inorg. Chim. Acta* **2013**, *405*, 374. (b) Calvo, B.; Davidson, M. G.; Garcia-Vivo, D. Polyamine-Stabilized Sodium Aryloxides: Simple Initiators for the Ring-Opening Polymerization of *rac*-Lactide. *Inorg. Chem.* **2011**, *50*, 3589.

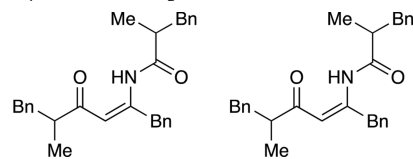
(28) Collum, D. B.; McNeil, A. J.; Ramirez, A. Lithium Diisopropylamide: Solution Kinetics and Implications for Organic Synthesis. *Angew. Chem., Int. Ed.* **2007**, *46*, 3002.

(29) Casado, J.; Lopez-Quintela, M. A.; Lorenzo-Barral, F. M. The Initial Rate Method in Chemical Kinetics: Evaluation and Experimental Illustration. *J. Chem. Educ.* **1986**, *63*, 450.

(30) We define the idealized rate law as that obtained by rounding the observed reaction orders to the nearest rational order.

(31) For an excellent review of enolate quaterization including several examples involving oxazolidinones, see: Minko, Y.; Marek, I. Stereodefined acyclic trisubstituted metal enolates towards the asymmetric formation of quaternary carbon stereocenters. *Chem. Commun.* **2014**, *50*, 12597.

(32) The backbone metalation product was obtained at a roughly 50% yield and characterized by various ^1H and ^{13}C NMR correlation spectroscopies to be the structure below. It appears to derive from deprotonation of auxiliary oxygen-neighboring methylene proton followed by acylation at that position.



(33) Schmidt, B.; Wildemann, H. Synthesis of enantiomerically pure divinyl- and diallylcarbinols. *J. Chem. Soc., Perkin Trans.* **2002**, *1*, 1050.

(34) LiHMDS has been shown to be substantially more reactive in Et_3N /toluene than in THF solution: Zhao, P.; Collum, D. B. Ketone Enolization by Lithium Hexamethyldisilazide: Structural and Rate

Studies of the Accelerating Effects of Trialkylamines. *J. Am. Chem. Soc.* **2003**, *125*, 14411.

(35) The oxazolidinone–NaHMDS complex in Et₃N/toluene shows IR absorbances at 1761 and 1711 cm⁻¹.

(36) Addition of BF₃ to accelerate organolithium-based epoxide cleavages was first reported by Ganem and coworkers: Eis, M. J.; Wrobel, J. E.; Ganem, B. Mechanism and Synthetic Utility of Boron Trifluoride Etherate-Promoted Organolithium Additions. *J. Am. Chem. Soc.* **1984**, *106*, 3693.

(37) Velazquez, F.; Olivo, H. The application of Chiral Oxazolidinethiones and thiazolidinethiones in Asymmetric Synthesis. *Curr. Org. Chem.* **2002**, *6*, 303.

(38) Azaaldol additions using Evans enolates: (a) Bian, J.; Blakemore, D.; Warmus, J. S.; Sun, J.; Corbett, M.; Rose, C. R.; Bechle, B. M. Diastereoselective Synthesis of β -Heteroaryl *syn*- α -Methyl- β -Amino Acid Derivatives via a Double Chiral Auxiliary Approach. *Org. Lett.* **2013**, *15*, 562. (b) Ma, Z.; Zhao, Y.; Jiang, N.; Jin, X.; Wang, J. Stereoselective Nucleophilic Addition of Chiral Lithium Enolates to (*N*-tosyl)Imines: Enantioselective Synthesis of β -Aryl- β -amino acid Derivatives. *Tetrahedron Lett.* **2002**, *43*, 3209.

(39) Azaaldols of alkali metal enolates to phenethylamines: Evans, C. D.; Mahon, M. F.; Andrews, P. C.; Muir, J.; Bull, S. D. Intramolecular Ester Enolate-Imine Cyclization Reactions for the Asymmetric Synthesis of Polycyclic β -Lactams and Cyclic β -Amino Acid Derivatives. *Org. Lett.* **2011**, *13*, 6276.

(40) (a) Vemula, R.; Wilde, N. C.; Goreti, R.; Corey, E. J. A New, Short, and Stereocontrolled Synthesis of C₂-Symmetric 1,2-Diamines. *Org. Lett.* **2017**, *19*, 3883. (b) Díez, R.; Badorrey, R.; Díaz-de-Villegas, M. D.; Gálvez, J. A. Highly Stereoselective Synthesis of Stereochemically Defined Polyhydroxylated Propargylamines by Alkynylation of *N*-Benzylimines Derived from (*R*)-Glyceraldehyde. *Eur. J. Org. Chem.* **2007**, *13*, 2114. (c) Kawate, T.; Yamada, H.; Yamaguchi, K.; Nishida, A.; Nakagawa, M. Asymmetric Additions of Alkylolithium to Chiral Imines – α -Naphthylethyl Group as a Chiral Auxiliary. *Chem. Pharm. Bull.* **1996**, *44*, 1776.

(41) Ma, Y.; Lobkovsky, E.; Collum, D. B. BF₃-Mediated Additions of Organolithiums to Ketimines: X-ray Crystal Structures of BF₃-Ketimine Complexes. *J. Org. Chem.* **2005**, *70*, 2335.

(42) The methyl stemming from the propionyl group appears as a broad “singlet” in the ¹H NMR spectrum at room temperature. Raising the temperature causes considerable sharpening around 40 °C, affording the anticipated doublet at 60 °C. Lowering the temperature to – 80 °C reveals two conformers attributed to hydrogen bonding. Despite the gamut of two-dimensional ¹H and ¹³C NMR spectroscopies, the assignment was ultimately made by derivatizing **22** as the corresponding BOC-protected methyl ester and comparing it with an authentic sample: Seebach, D.; Abele, S.; Gademann, K.; Guichard, G.; Hintermann, T.; Jaun, B.; Mathews, J. L.; Schreiber, J. V. β^2 and β^3 -Peptides with Proteinaceous Side Chains: Synthesis and solution structures of constitutional isomers, a novelhelical hydrophobic interactions on folding. *Helv. Chim. Acta* **1998**, *81*, 932.

(43) (a) Vemula, R.; Wilde, N. C.; Goreti, R.; Corey, E. J. A New, Short, and Stereocontrolled Synthesis of C₂-Symmetric 1,2-Diamines. *Org. Lett.* **2017**, *19*, 3883. (b) Vieth, U.; Leurs, S.; Jäger, V. Auxiliary-controlled diastereoselection by *N*-(1-phenylethyl) in Grignard additions to 2-*O*-benzyglyceraldehyde imines. *Chem. Commun.* **1996**, *3*, 329. (c) Chandrasekhar, S.; Pendke, M.; Muththe, C.; Akondi, S. M.; Mainkar, P. S. Synthesis of α,α -dideutero- β -amino esters. *Tetrahedron Lett.* **2012**, *53*, 1292.

(44) After several abortive attempts to ascertain the optical purity of **25** using HPLC and NMR shift reagents, reaction with the lithium salt of the oxazolidinone auxiliary afforded aldol adduct **23** contaminated by the other *syn* isomer (7:1) albeit in low (15%) yield.

(45) (a) Gruver, J. M.; Liou, L. R.; McNeil, A. J.; Ramírez, A.; Collum, D. B. Solution Structures of Lithium Enolates, Phenolates, Carboxylates, and Alkoxides in the Presence of *N,N,N',N'*-Tetramethylethylenediamine: A Prevalence of Cyclic Dimers. *J. Org. Chem.* **2008**, *73*, 7743. (b) Liou, L. R.; McNeil, A. J.; Ramírez, A.;

Toombes, G. E. S.; Gruver, J. M.; Collum, D. B. Lithium Enolates of Simple Ketones: Structure Determination Using the Method of Continuous Variation. *J. Am. Chem. Soc.* **2008**, *130*, 4859.

(46) (a) Ashby, M. T.; Govindan, G. N.; Grafton, A. K. Kinetics and Mechanism of the Facile Diastereomeric Isomerization of a Tris(bidentate)ruthenium(II) Complex Bearing a Misdirected Bipyridyl Ligand: Δ/Λ -(δ/λ -1,1'-Biisoquinoline)bis(2,2'-bipyridine)-ruthenium(II). *Inorg. Chem.* **1993**, *32*, 3803. (b) Barton, J. K.; Danishefsky, A. T.; Goldberg, J. M. Tris(phenanthroline)ruthenium-(II): Stereoselectivity in Binding to DNA. *J. Am. Chem. Soc.* **1984**, *106*, 2172. (c) Haq, I.; Lincoln, P.; Suh, D.; Norden, B.; Chowdhry, B. Z.; Chaires, J. B. Interaction of Δ - and Λ -[Ru(phen)₂DPPZ]²⁺ with DNA: A Calorimetric and Equilibrium Binding Study. *J. Am. Chem. Soc.* **1995**, *117*, 4788.

(47) Bauer, W.; Schleyer, P. v. R. In *Advances in Carbanion Chemistry*; Snieckus, V., Ed.; JAI: New York, 1992; p 89.

(48) (a) Edmonds, M. K.; Graichen, F. H. M.; Gardiner, J.; Abell, A. D. Enantioselective Synthesis of α -Fluorinated β^2 -Amino Acids. *Org. Lett.* **2008**, *10*, 885. (b) Peddie, V.; Pietsch, M.; Bromfield, K. M.; Pike, R. N.; Duggan, P. J.; Abell, A. D. Fluorinated β^2 - and β^3 -amino acids: synthesis and inhibition of α -chymotrypsin. *Synthesis* **2010**, *11*, 1845. (c) Falck, J. R.; Gao, S.; Prasad, R. N.; Koduru, S. R. Electrophilic α -thiocyanation of chiral and achiral *N*-acyl imides. A convenient route to 5-substituted and 5, 5-disubstituted 2, 4-thiazolidinediones. *Bioorg. Med. Chem. Lett.* **2008**, *18*, 1768. (d) Minko, Y.; Marek, I. Stereodefined acyclic trisubstituted metal enolates towards the asymmetric formation of quaternary carbon stereocentres. *Chem. Commun.* **2014**, *50*, 12597 and references cited therein .

(49) Fuerstner, A.; Fenster, M. D. B.; Fasching, B.; Godbout, C. P.; Radkowski, K. Toward the total synthesis of spirastrellolide A. Part 2: Conquest of the northern hemisphere. *Angew. Chem., Int. Ed.* **2006**, *45*, 5510.

(50) Li, B.-J.; El-Nachef, C.; Beauchemin, A. M. Organocatalysis using aldehydes: the development and improvement of catalytic hydroaminations, hydrations and hydrolyses. *Chem. Commun.* **2017**, *53*, 13192.

(51) (a) Koskinen, A. M. P.; Kataja, A. O. The Tishchenko Reaction. *Org. React.* **2015**, *86*, 105. (b) Mahrwald, R. In *Modern Aldol Reactions*; Mahrwald, R., Ed.; Wiley-VCH: Weinheim, 2004; Vol. 2, p 327.

(52) Algera, R. F.; Ma, Y.; Collum, D. B. Sodium Diisopropylamide in Tetrahydrofuran: Selectivities, Rates, and Mechanisms of Arene Metalations. *J. Am. Chem. Soc.* **2017**, *139*, 15197.

(53) (a) Ojeda-Amador, A. I.; Martinez-Martinez, A. J.; Kennedy, A. R.; O'Hara, C. T. Synthetic and structural studies of mixed sodium bis(trimethylsilyl) amide/sodium halide aggregates in the presence of η^2 -*N,N,N'*, η^3 -*N,N,N,N,O,N'*, and η^4 -*N,N,N,N,N'*-donor ligands. *Inorg. Chem.* **2015**, *54*, 9833. (b) For a NaHMDS-sodium enolate mixed aggregate characterized crystallographically, see: Williard, P. G.; Hintze, M. J. Mixed Aggregates: Crystal Structures of a Lithium Ketone Enolate/Lithium Amide and of a Sodium Ester Enolate/Sodium Amide. *J. Am. Chem. Soc.* **1990**, *112*, 8602.

(54) Mixed aggregation can tip the relative contributions of competing monomer- and dimer-based toward the monomer through the net dilution of the homoaggregates: Ramírez, A.; Sun, X.; Collum, D. B. Lithium Diisopropylamide-Mediated Enolization: Catalysis by Hemilabile Ligands. *J. Am. Chem. Soc.* **2006**, *128*, 10326.

(55) For a discussion of aggregation and cooperative effects on the aldol addition, see: Larranaga, O.; de Cozar, A.; Bickelhaupt, F. M.; Zangi, R.; Cossio, F. P. Aggregation and cooperative effects in the aldol reactions of lithium enolates. *Chem. - Eur. J.* **2013**, *19*, 13761.

(56) Oxazolidinone precursors to enolates **2**, **9a–e**, and **10** were prepared according to literature procedures. (a) Mabe, P. J.; Zakarian, A. Asymmetric radical addition of TEMPO to titanium enolates. *Org. Lett.* **2014**, *16*, 516. (b) Kretschmer, M.; Dieckmann, M.; Li, P.; Rudolph, S.; Herkommer, D.; Troendlin, J.; Menche, D. Modular Total Synthesis of Rhizopodin: A Highly Potent G-Actin Dimerizing Macrolide. *Chem. - Eur. J.* **2013**, *19*, 15993. (c) Szostak, M.; Spain, M.;

Eberhart, A. J.; Procter, D. J. Highly chemoselective reduction of amides (primary, secondary, tertiary) to alcohols using SmI₂/amine/H₂O under mild conditions. *J. Am. Chem. Soc.* **2014**, *136*, 2268. (d) Gille, A.; Hiersemann, M. (–)-Lytophilippine A: Synthesis of a C1–C18 Building Block. *Org. Lett.* **2010**, *12*, 5258. (e) Bull, S. D.; Davies, S. G.; Jones, S.; Sanganee, H. J. Asymmetric alkylations using SuperQuat auxiliaries—an investigation into the synthesis and stability of enolates derived from 5, 5-disubstituted oxazolidin-2-ones. *J. Chem. Soc., Perkin Trans. 1* **1999**, *4*, 387. (57) Kummer, D. A.; Chain, W. J.; Morales, M. R.; Quiroga, O.; Myers, A. G. Stereocontrolled alkylative construction of quaternary carbon centers. *J. Am. Chem. Soc.* **2008**, *130*, 13231.